






Cerebrovascular Function in Sporadic and Genetic Cerebral Small Vessel Disease

Michael S. Stringer, PhD  ¹ Gordon W. Blair, PhD,¹ Anna Kopczak, MD ²
Danielle Kerkhofs, PhD,³ Michael J. Thrippleton, PhD,¹ Francesca M. Chappell, PhD,¹
Susana Muñoz Maniega, PhD,¹ Rosalind Brown, PhD,¹ Kirsten Shuler, PhD,¹
Iona Hamilton, BSc,¹ Daniela Jaime Garcia, MSc,¹ Fergus N. Doubal, PhD,¹
Una Clancy, PhD,¹ Eleni Sakka, MSc,¹ Tetiana Poliakova, MSc,¹ Esther Janssen, PhD,¹
Marco Duering, MD,^{2,4} Michael Ingris, PhD,⁵ Julie Staals, PhD,³
Walter H. Backes, PhD ⁶, Robert van Oostenbrugge, PhD,³ Geert Jan Biessels, PhD,⁷
Martin Dichgans, MD,^{2,8,9} and Joanna M. Wardlaw, MD, ¹ The SVDs@target consortium

Objective: Cerebral small vessel diseases (SVDs) are associated with cerebrovascular dysfunction, such as increased blood–brain barrier leakage (permeability surface area product), vascular pulsatility, and decreased cerebrovascular reactivity (CVR). No studies assessed all 3 functions concurrently. We assessed 3 key vascular functions in sporadic and genetic SVD to determine associations with SVD severity, subtype, and interrelations.

Methods: In this prospective, cross-sectional, multicenter INVESTIGATE-SVDs study, we acquired brain magnetic resonance imaging in patients with sporadic SVD/cerebral autosomal dominant arteriopathy with subcortical infarcts and leukoencephalopathy (CADASIL), including structural, quantitative microstructural, permeability surface area product, blood plasma volume fraction, vascular pulsatility, and CVR (in response to CO₂) scans. We determined vascular function and white matter hyperintensity (WMH) associations, using covariate-adjusted linear regression; normal-appearing white matter and WMH differences, interrelationships between vascular functions, using linear mixed models; and major sources of variance using principal component analyses.

Results: We recruited 77 patients (45 sporadic/32 CADASIL) at 3 sites. In adjusted analyses, patients with worse WMH had lower CVR ($B = -1.78$, 95% CI $-3.30, -0.27$) and blood plasma volume fraction ($B = -0.594$, 95% CI $-0.987, -0.202$). CVR was worse in WMH than normal-appearing white matter (eg, CVR: $B = -0.048$, 95% CI $-0.079, -0.017$). Adjusting for WMH severity, SVD subtype had minimal influence on vascular function (eg, CVR in CADASIL vs sporadic: $B = 0.0169$, 95% CI $-0.0247, 0.0584$). Different vascular function mechanisms were not generally interrelated (eg, permeability surface area product~CVR: $B = -0.85$, 95% CI $-4.72, 3.02$). Principal component analyses identified WMH volume/quantitative microstructural metrics explained most variance in CADASIL and arterial pulsatility in sporadic SVD, but similar main variance sources.

View this article online at [wileyonlinelibrary.com](https://onlinelibrary.wiley.com/doi/10.1002/ana.27136). DOI: 10.1002/ana.27136

Received Jun 8, 2024, and in revised form Oct 28, 2024. Accepted for publication Oct 28, 2024.

Address correspondence to Prof Wardlaw, Neuroimaging Science, Centre for Clinical Brain Science, University of Edinburgh, 49 Little France Crescent, Edinburgh, EH164SB, UK. E-mail: joanna.wardlaw@ed.ac.uk

Registration: URL: <https://www.isrctn.com/>; Unique identifier: ISRCTN10514229.

From the ¹Brain Research Imaging Center, Center for Clinical Brain Sciences, UK Dementia Institute Center at the University of Edinburgh, Edinburgh, UK;

²Institute for Stroke and Dementia Research (ISD), University Hospital, Munich, Germany; ³Department of Neurology, CARIM School for cardiovascular diseases, Maastricht University Medical Center, Maastricht, the Netherlands; ⁴Medical Image Analysis Center (MIAC AG) and Department of Biomedical Engineering, University of Basel, Basel, Switzerland; ⁵Department of Radiology, University Hospital, Munich, Germany; ⁶Department of Radiology & Nuclear Medicine, Maastricht University Medical Center, Schools for Mental Health & Neuroscience and Cardiovascular Disease, Maastricht, the Netherlands; ⁷Department of Neurology and Neurosurgery, UMC Utrecht Brain Center, University Medical Center Utrecht, Utrecht, Netherlands; ⁸German Center for Neurodegenerative Diseases (DZNE, Munich), Munich, Germany; and ⁹Munich Cluster for Systems Neurology (SyNergy), Munich, Germany

Additional supporting information can be found in the online version of this article.

Interpretation: Vascular function was worse with higher WMH, and in WMH than normal-appearing white matter. Sporadic SVD-CADASIL differences largely reflect disease severity. Limited vascular function interrelations may suggest disease stage-specific differences.

ANN NEUROL 2025;97:483–498

Cerebral small vessel diseases (SVDs) cause one-quarter of ischemic strokes and up to 50% of dementias, either vascular or mixed.¹ Sporadic SVD, the commonest type that may be covert, or cause stroke, cognitive impairment, or mobility or mood problems, increases with age.² Genetic SVDs, including cerebral autosomal dominant arteriopathy with subcortical infarcts and leukoencephalopathy (CADASIL), are typically more severe, usually affecting younger adults.

Hypertension is the major modifiable risk factor for sporadic SVD.³ However, apart from vascular risk factor management, which has rather limited effect on preventing adverse outcomes,⁴ as yet there are no specific therapies for SVDs, possibly reflecting incomplete understanding of its pathophysiology.¹

Sporadic and genetic SVDs cause similar types of lesions on brain magnetic resonance imaging (MRI), primarily white matter hyperintensities (WMH), but also lacunes, microbleeds, and increased perivascular space visibility.⁵ SVDs lesions are considered “ischemic” based on pathological studies, but these typically reflect end-stage damage. Key cerebrovascular mechanisms can be assessed in vivo using MRI, including blood–brain barrier (BBB) leakage using gadolinium-based contrast agents,⁶ cerebrovascular reactivity (CVR) as the response to CO₂ during blood oxygen level-dependent (BOLD) MRI,^{7,8} and venous/arterial pulsatility with phase contrast MRI (PC-MRI).⁹

In vivo studies in sporadic SVD using these MRI techniques have shown that more severe SVD is associated with subtle BBB leakage,^{10,11} impaired CVR,^{12,13} and higher blood pulsatility index.⁹ However, there have been few studies in genetic SVD,¹¹ and no studies investigated these different aspects of cerebrovascular function simultaneously in the same patients.¹⁴

We established the prospective multisite Imaging NeuroVascular, Endothelial and STructural InteGritY in prepAration to TrEat Small Vessel Diseases (INVESTIGATE-SVDs) study to determine which of the 3 main vascular function metrics (BBB leakage, CVR, blood pulsatility) were most closely related to SVD severity, and whether the underlying function differed between sporadic SVD and CADASIL. We hypothesized that the 3 cerebrovascular functions would be the most abnormal in patients with the worst WMH burden, and that a similar pattern of more BBB leakage, lower CVR, and higher pulsatility would occur in sporadic SVD and CADASIL.

Methods

Regulatory Approvals

INVESTIGATE-SVDs received ethical approval at Edinburgh (South East Scotland Research Ethics Committee, Reference 16/SS/0123), Maastricht (Medical Ethical Committee of Maastricht University Medical Center, Reference 16–2044), and Munich (Ethics Committee of the LMU Munich, Reference 658–16).¹⁴ All participants provided written informed consent. INVESTIGATE-SVDs is registered (ISRCTN 10514229), and followed the STROBE Guidelines.

Patients

We recruited participants aged ≥18 years with capacity to consent and independent in activities of daily living (modified Rankin score <3) from stroke or specialist genetic SVD clinics who presented with either a lacunar stroke in the past 5 years with a corresponding small subcortical infarct on MRI or computed tomography at presentation, or a formal diagnosis of CADASIL. We excluded participants with other major neurological or psychiatric conditions affecting the brain and interfering with the study design (eg, multiple sclerosis); other causes of stroke (eg, ≥50% luminal stenosis in large arteries supplying the area of ischemia); major-risk cardioembolic source of embolism; other specific causes of stroke identified (eg, hemorrhage, arteritis, dissection etc.) and other stroke risk factor requiring immediate intervention precluding study participation; and contraindications to MRI, gadolinium-based contrast agents or CO₂ challenge (eg, severe respiratory disease).¹⁴ No healthy control group was acquired, as a healthy control group does not account for medication effects, co-existing conditions such as hypertension, and the high prevalence of SVD in older age.¹ Instead, we concentrated on gathering a broad spread of disease burdens. The study protocol, including full inclusion and exclusion criteria, is published elsewhere.¹⁴

Clinical Assessment

Before brain MRI, we recorded SVD-related clinical features (eg, diagnosis date, presenting symptoms, relevant investigations), vascular risk factors (diagnosis of hypertension, hyperlipidemia, diabetes, smoking status), past medical history, and current prescribed medications. We measured resting blood pressure (BP) while seated, pulse, height, and weight.

Telemetric BP

All participants recorded their BP at home for 7 days before MRI using a validated, CE-marked telemetric BP device (Tel-O-Graph; IEM GmbH, Stolberg, Germany),¹⁵ taking 2 consecutive readings while seated 3 times per day (on waking, at midday, and before bed).¹⁴ Readings were transferred telemetrically to a central database in Munich.

We calculated BP variability (BPV)^{16,17} from the telemetric BP data as the coefficient of variation (standard deviation/mean) using second readings on waking, around lunch time, and before bed, using an in-house MATLAB script. Full details have been previously described.^{14,18}

MRI Acquisition

Participants underwent the same structural and vascular function 3 Tesla brain MRI protocol at all 3 sites on Siemens Prisma scanners (Siemens Healthcare, Erlangen, Germany; apart from the first 3 scans in Munich, which were acquired on a Siemens Skyra). Full details are published,^{14,18} including the quality assurance program (Supplementary Methods S1 and Table 1), and can be downloaded at <https://harness-neuroimaging.org>. All imaging protocols^{7,9,19,20} followed consensus recommendations.⁶ The protocol included:

- Structural imaging 3D T1-weighted, T2-weighted (T2-w), fluid attenuated inversion recovery, and susceptibility-weighted imaging to assess disease burden and measure brain volumes;
- Multi-shell diffusion imaging (dMRI) to quantify white matter microstructure;
- Quantitative T_1 relaxation time to assess tissue water content, and to use in the BBB permeability calculations;
- Dynamic contrast-enhanced MRI (DCE-MRI) with 0.1 mmol/kg bodyweight intravenous gadobutrol (1 M Gadovist; Bayer AG, Leverkusen, Germany) to assess BBB leakage (permeability surface area product [PS]) and blood plasma volume fraction (v_p);
- Phase contrast (PC) MRI to assess blood flow and pulsatility in the internal carotid and vertebral arteries, internal jugular veins, straight, sagittal and transverse venous sinuses, and cerebrospinal fluid at the foramen magnum;
- Dynamic BOLD sequence during alternating inspiration of 2 minutes medical air (21:79 O₂:N₂) and 3 minutes 6% CO₂ (balance 21:73 O₂:N₂, 2 cycles) delivered from gas cylinders to measure CVR using a proven reproducible paradigm suitable for patients with SVD that gives a robust response of cerebral

microvessels while allowing natural, unforced respiration.^{7,18}

MRI Quality Assurance

We performed regular quality assurance using phantoms and volunteers throughout the study to monitor scanner stability and acquisitions, and ensure data consistency (see Supplementary Methods/Quality assurance).

MRI Processing and Analysis

All imaging data were anonymized and transferred securely to Edinburgh using established protocols (<https://www.ed.ac.uk/clinical-sciences/edinburgh-imaging/research/services-and-collaboration/smartis>). All analyses used validated methods,¹⁴ were blinded to all other measures, and visually checked for accuracy, briefly summarized here (full details of image processing including region of interest determination, dMRI, T_1 relaxation time, and vascular function measures are in Supplementary Materials and the published protocol¹⁴).

SVD Features Visual Assessment. We rated structural images for SVD features using the STRIVE-1 criteria⁵ (E.J., J.M.W.). We scored WMHs using the Fazekas scale,²¹ summing periventricular and deep WMH scores to give a score from 0 to 6; perivascular spaces (PVS) using a validated, semiquantitative ordinal scale (range 0–4) summing basal ganglia and centrum semiovale scores⁵; presence/absence and total number of microbleeds; and determined brain atrophy score (range 1–6) with reference to a normal aging template.²²

Whole and Subregional Brain and WMH Volumes Segmentation. We co-registered structural images to the T2-w images using FLIRT.²³ We determined intracranial volume by extracting²⁴ the brain from the magnitude susceptibility-weighted imaging. We (M.S.) manually delineated and excluded stroke lesions according to STRIVE-1 guidelines⁵ with neuroradiological supervision (J.M.W.).

We assessed vascular function in normal-appearing white matter (NAWM), subcortical gray matter (SGM), and WMH regions of interest. We segmented SGM using FIRST,²⁵ combining the caudate, putamen, pallidum, and thalamus. We applied a validated semiautomatic technique to calculate WMH volumes based on intensity thresholding and a multispectral approach, and excluded stroke lesions.⁹ We segmented whole-brain NAWM and cerebrospinal fluid (including ventricles), using FAST.²⁶ We excluded WMH, SGM, brainstem, and stroke lesion masks from the NAWM mask, and WMH and stroke lesions from the SGM mask.

Table 1. Demographics, Blood Pressure, Small Vessel Diseases Lesion Visual Ratings, and Structural Brain Volumes.

	All patients	Sporadic SVD	CADASIL	Sporadic SVD versus CADASIL
Demographics				
Total, n (%)	77 (100)	45 (100)	32 (100)	
M/F, n (%)	42/35 (54.5/45.5)	26/19 (57.7/42.2)	16/16 (50.0/50.0)	$\chi^2 = 0.456, p = 0.50$
Age (yr)	59.5 \pm 12.3 (23.6–87.0)	64.2 \pm 11.0 (43.0–87.0)	52.9 \pm 11.1 (23.6–70.0)	$t = 4.44, 95\% \text{ CI} = 6.24, 16.4$
Diabetes	10 (13.0)	9 (20.0)	1 (3.1)	$p = 0.039$
Hypertension	46 (59.7)	35 (77.7)	11 (34.4)	$\chi^2 = 14.6, p < 0.001$
Hyperlipidemia	46 (59.7)	33 (73.3)	13 (40.6)	$\chi^2 = 8.32, p = 0.004$
Current & ex-smoker	41 (53.3)	23 (51.1)	18 (56.3)	$\chi^2 = 0.198, p = 0.66$
Does use alcohol	55 (71.4)	31 (68.8)	24 (75.0)	$\chi^2 = 0.342, p = 0.56$
Alcohol units /week	1 (0–5)	2 (0–7)	1 (0.5–2.5)	$t = 1.01, 95\% \text{ CI} = -9.67, 2.97$
Blood pressure				
Pre-CVR systolic (mmHg)	143.6 \pm 24.3 (90.0–200.0)	156.7 \pm 23.2 (90.0–200.0)	127.7 \pm 13.9 (110.0–160.0)	$t = 6.53, 95\% \text{ CI} = 20.1, 37.9$
Pre-CVR diastolic (mmHg)	82.2 \pm 12.3 (50.0–110.0)	86.7 \pm 12.7 (50.0–110.0)	76.7 \pm 9.5 (60.0–90.0)	$t = 3.81, 95\% \text{ CI} = 4.78, 15.3$
Mean 24-h systolic (mmHg)	125.0 \pm 12.3 (100.7–157.1)	130.3 \pm 11.6 (105.7–157.1)	117.5 \pm 9.1 (100.7–139.9)	$t = 5.40, 95\% \text{ CI} = 8.04, 17.4$
Mean 24-h diastolic (mmHg)	80.4 \pm 9.5 (60.6–105.4)	83.0 \pm 9.13 (62.4–105.4)	76.7 \pm 8.9 (60.6–90.2)	$t = 3.08, 95\% \text{ CI} = 2.24, 10.5$
Systolic BPV (unit less)	0.0750 \pm 0.0229 (0.0321–0.1493)	0.0821 \pm 0.0241 (0.0340–0.1493)	0.0651 \pm 0.0169 (0.0321–0.1063)	$t = 3.66, 95\% \text{ CI} = -0.008, 0.0264$
Diastolic BPV (unit less)	0.0801 \pm 0.0235 (0.0362–0.1444)	0.0804 \pm 0.0214 (0.0488–0.1444)	0.0796 \pm 0.0266 (0.0362–0.1400)	$t = 0.14, 95\% \text{ CI} = -0.011, 0.012$
Visual SVD ratings				
Total Fazekas	4 (3–6)	3 (2–4)	6 (5–6)	$W = 1856, p < 0.0001$
Total PVS	5 (3–6)	4 (3–5)	6 (4–8)	$W = 1,641, p = 0.0001$
No. of lacunes	3 (0–7)	1 (0–4)	5.5 (1–9)	$W = 1,524, p = 0.0051$
No. of microbleeds	0 (0–4)	0 (0–1)	1.5 (0–8)	$W = 1,474, p = 0.0134$
Deep atrophy score	3 (3–4)	4 (3–5)	3 (2–3)	$W = 1,007, p = 0.012$
Superficial atrophy score	3 (3–4)	4 (3–4)	3 (2–4)	$W = 1,103, p = 0.13$
Intracranial volume (ml)	1413.03 \pm 133.37 (1142.07–1878.32)	1425.49 \pm 151.52 (1180.12–1878.32)	1395.51 \pm 102.39 (1142.07–1603.28)	$t = 1.04, 95\% \text{ CI} = -27.7, 87.6$
Brain volume (ml)	1104.92 \pm 101.29 (881.47–1360.20)	1085.60 \pm 108.63 (881.47–1307.42)	1132.08 \pm 84.26 (963.88–1360.2)	$t = -2.11, 95\% \text{ CI} = -90.3, -2.64$
CSF volume (ml)	302.38 \pm 74.54 (172.04–609.08)	334.35 \pm 71.23 (219.21–609.08)	257.42 \pm 53.37 (172.04–362.92)	$t = 5.42, 95\% \text{ CI} = 48.6, 105$
GM volume (ml)	530.64 \pm 51.39 (411.65–679.04)	536.00 \pm 53.04 (421.61–679.04)	523.09 \pm 48.80 (411.65–629.02)	$t = 1.10, 95\% \text{ CI} = -10.4, 36.3$
NAWM volume (ml)	532.76 \pm 57.96 (421.07–701.99)	537.53 \pm 55.79 (432.54–655.42)	526.05 \pm 61.14 (421.07–701.99)	$t = 0.84, 95\% \text{ CI} = -15.8, 38.7$
WMH volume (ml)	14.63 (5.71–58.24)	7.94 (4.24–11.97)	69.88 (40.13–113.30)	$W = 1884, p < 0.0001$

All values reported as number (percentage) for categorical, mean \pm standard deviation (range) for normally distributed numeric variables, and median (interquartile range) otherwise. χ^2 for chi-squared, p for p value, t for t value, 95% CI for 95% confidence interval and W for Wilcoxon's rank sum. Fisher's exact test was used for diabetes. All statistical tests are unadjusted for covariates.

Abbreviations: BPV = blood pressure variability; CADASIL = cerebral autosomal dominant arteriopathy with subcortical infarcts and leukoencephalopathy; CSF = cerebrospinal fluid; CVR = cerebrovascular reactivity; GM = gray matter; NAWM = normal-appearing white matter; SVD = small vessel disease; WMH = white matter hyperintensity.

We eroded the SGM and NAWM masks inwards by 2 mm circumferentially to reduce partial volume effects while maximizing tissue retention. We did not erode the WMH mask to avoid excluding small punctate hyperintensities. As vessels running on the inner ventricular surface artefactually increase the BOLD signal, we dilated the ventricles to exclude adjacent periventricular tissue (whether NAWM or WMH) by 5 voxels (5 mm) left-right, and 4 voxels (4 mm) infero-superior and antero-posterior. For each participant, we registered and overlaid the resulting masks on the voxelwise CVR map to exclude “blooming artefacts” from large veins and venous sinuses. All masks were checked and manually edited as needed to avoid misclassification (see Supplementary Methods image processing).

Quantitative Tissue and Vascular Function Metrics. Using validated established techniques, we processed the dMRI, quantitative T_1 ,^{19,27} DCE-MRI, PC-MRI, and CVR^{6,7,9} data for each region of interest (details in supplement). We did not perform voxelwise analyses, as the contrast-to-noise ratio for the BOLD and DCE-MRI^{6,7} signals are generally low.

Statistical Analysis

We reported all data for all available participants. We calculated summary statistics as the mean \pm standard deviation and (range)/median (interquartile range) for normally/non-normally distributed continuous data respectively, and proportions for count data. We used histograms/bar charts for univariate plots and scatterplots for bivariate relationships. We used \log_{10} of WMH volume standardized to intracranial volume to account for head size and meet linear regression assumptions. For unadjusted (univariate) comparisons, we reported χ^2 -tests as χ^2 , 95% confidence intervals (95% CI), p values for binary/unpaired categorical data, and used Fisher’s exact test (p -value) where there were insufficient values (<5); t tests as t value, 95% CI, p value for continuous variables; and Wilcoxon’s rank sum, p -value for non-parametric data.

We report descriptive results for BP measures and diagnosis of hypertension. Based on previous studies,^{16,17} we used systolic BPV in analyses.

We used multivariable linear regression to assess the association between WMH volume and vascular function metrics measured in NAWM and WMH, using separate models adjusted for key vascular risk factors (age, smoking status [0 = never, 1 = current/ever smoker], SVD subtype, and systolic BPV). We chose these risk factors as they are known important WMH predictors. We limited the number of risk factors to avoid overfitting and poor

generalizability.²⁸ We report unstandardized coefficients (B), 95% CI, and p value.

We used linear mixed models to examine how vascular function metrics measured in NAWM and WMH interrelated and differed between the two tissues adjusted for the aforementioned co-variables (age, smoking status, SVD subtype, and systolic BPV), the remaining vascular function metrics, with an interaction term for tissue type (NAWM/WMH) and WMH volume, with participant ID as a random effect. We tested CVR, v_p and BBB PS as the outcomes. The coefficient for outcome~WMH volume is given for NAWM; to obtain the coefficient for WMH, the interaction term effect is added. Excluding WMH volume would have biased the coefficient estimates. For all models, we considered the direction of effect of the point estimate, breadth of the confidence interval, and existing clinical knowledge rather than solely p values when assessing and interpreting relationships between variables.^{29,30}

Finally, we conducted a principal components analysis (PCA), an unsupervised data-reduction technique that seeks to identify the main sources of variance in the data by grouping related variables into “latent factors” that each explain part of the variance in the data.³¹ Each “latent factor” was then ranked according to the proportion of variance it explained in the whole dataset. We report only factors that explained more variance than random noise, decided using scree and parallel line plots. We examined the whole dataset first, then examined the CADASIL and sporadic SVD participants separately in sensitivity analyses.

For all analyses, we checked underlying statistical assumptions and removed predictors causing collinearity, as assessed using variance inflation factors, where necessary. We rescaled mean diffusivity (MD; $\times 1,000$), PS ($\times 10,000$), and v_p ($\times 100$) for range consistency with other variables to avoid introducing collinearity.

We used SAS 9.4 (www.sas.com) for regression analyses and PCA, and R 3.6.2 (<https://cran.r-project.org>) for graphs.

Results

Patient Characteristics

We recruited 77 patients; 45 with sporadic SVD (25 at Edinburgh, 20 at Maastricht) and 32 with CADASIL (at Munich). All patients provided complete, analyzable structural imaging, but 7 CVR, 4 dMRI, 1 PC-MRI, 2 quantitative T_1 , and 9 DCE-MRI scans were not analyzable (reasons in Supplementary Figure S2).

The 77 patients had a mean age of 59.5 ± 12.3 years (23.6–87.0 years), 35 were women, 60% had hypertension,

60% hyperlipidemia, 13% diabetes, and 53% were current/ex-smokers (Table 1). Patients with sporadic SVD were older ($t = 4.4$, 95% CI 6.2, 16.4, $p < 0.001$) and more often had diabetes (Fisher's, 95% CI 3.7, 30.0, $p = 0.039$), hypertension ($\chi^2 = 14.6$, 95% CI 22.9, 63.9, $p < 0.001$), and hyperlipidemia ($\chi^2 = 8.3$, 95% CI 11.3, 54.1, $p = 0.004$) than those with CADASIL.

The mean telemetric BP was 125.0 ± 12.3 mmHg (100.7–157.1 mmHg) systolic and 80.4 ± 9.5 mmHg (60.6–105.4 mmHg) diastolic. Systolic BP ($t = 5.4$, 95% CI 8.0–17.4, $p < 0.0001$), diastolic BP ($t = 3.1$, 95% CI 2.2, 10.5, $p = 0.003$), systolic BPV ($t = -0.0171$, 95% CI 0.0078, 0.0264, $p = 0.0005$), and MRI visit BP measurements (Table 1) were higher in patients with sporadic SVD than CADASIL.

The median total Fazekas score was 4 (3–6), 48 patients (62%) had moderate–severe WMH (Fazekas ≥ 4), the median total PVS score was 5 (3–6), and number of lacunes 3 (0–7) and microbleeds was 0 (0–4); 54 (70%) patients had lacunes and 36 (47%) had microbleeds. All SVD features were worse in patients with CADASIL than sporadic SVD (Table 1, Fig 1 and S3);

for example, WMH volume CADASIL 69.9 ml (40.1–113.3 ml), sporadic SVD 7.94 ml (4.2–12.0 ml); Wilcoxon 1884, $p < 0.0001$.

Vascular function and tissue structural imaging measures are shown in Table 2. In unadjusted comparisons, some measures were worse in patients with CADASIL than sporadic SVD; for example, MD was higher, fractional anisotropy (FA) and v_p lower in NAWM and WMH, and venous pulsatility lower in CADASIL versus sporadic SVD patients.

WMH Volume and Vascular Functions

Patients with higher WMH volumes had lower v_p ($B = -0.594$, 95% CI -0.987 , -0.202 , $p = 0.0037$), lower CVR ($B = 1.78$, 95% CI -3.30 , -0.27 , $p = 0.02$), and a tendency to higher arterial ($B = 0.119$, 95% CI -0.127 , 0.365 , $p = 0.34$), venous pulsatility ($B = 0.116$, 95% CI -0.567 , 0.799 , $p = 0.73$), and higher PS ($B = 0.010$, 95% CI -0.075 , 0.095 , $p = 0.82$) in WMH, with a broadly similar pattern in NAWM (Table 3, Fig 2).

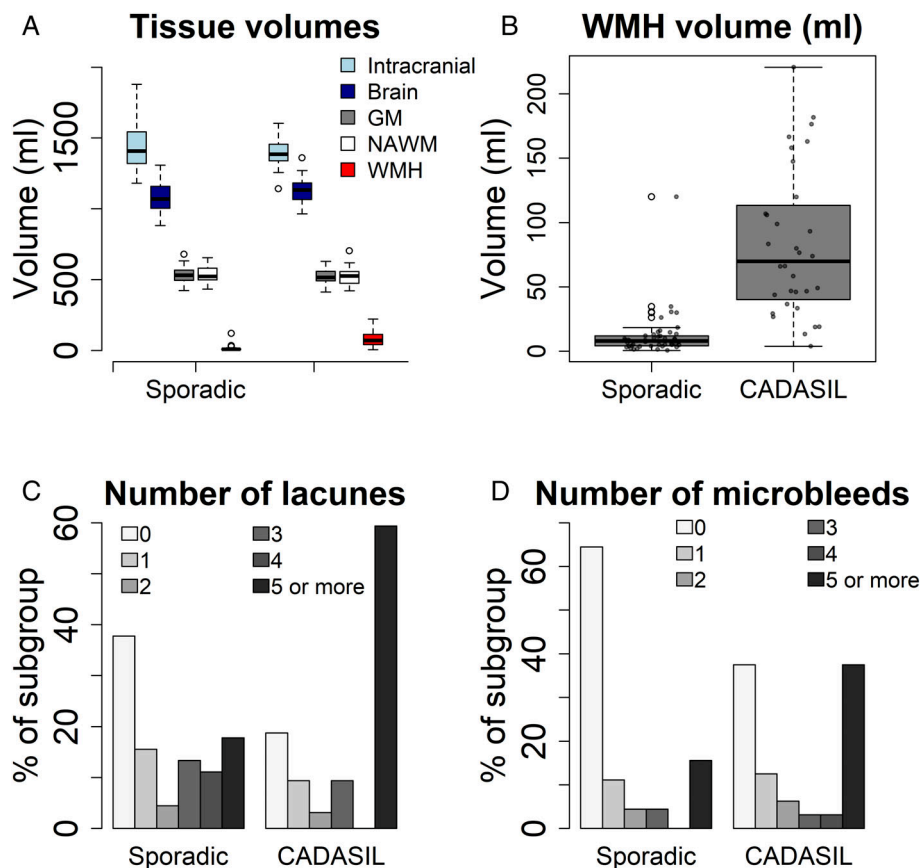


Figure 1: Panel showing key imaging characteristics by small vessel disease subtype. (A) Tissue volumes (ml), (B) white matter hyperintensity (WMH) volume (ml), (C) number of lacunes, and (D) number of microbleeds. WMH, white matter hyperintensity volume. CADASIL = cerebral autosomal dominant arteriopathy with subcortical infarcts and leukoencephalopathy; GM = gray matter; NAWM = normal-appearing white matter.

Table 2. Vascular Function, Quantitative T_1 and Diffusion Imaging Metrics for All Patients and by Disease Subtype.

	All patients	Sporadic SVD	CADASIL	CADASIL versus sporadic SVD
Permeability surface area (10^{-4} min^{-1})				
Subcortical gray matter	0.90 ± 1.19 (-3.52–4.56)	0.97 ± 1.30 (-3.52–4.56)	0.80 ± 1.01 (-1.88–2.85)	$t = 0.62$, 95% CI = -0.38, 0.73
Normal-appearing white matter	0.25 ± 0.91 (-2.39–2.01)	0.23 ± 0.97 (-2.39–2.01)	0.29 ± 0.83 (-1.21–1.81)	$t = -0.28$, 95% CI = -0.50, 0.37
White matter hyperintensity	0.79 ± 1.05 (-2.39–3.14)	0.71 ± 1.17 (-2.39–3.14)	0.92 ± 0.84 (-1.57–2.63)	$t = -8.71$, 95% CI = -0.70, 0.27
Plasma volume (v_p, 10^{-2})				
Subcortical gray matter	1.27 ± 0.28 (0.62–1.79)	1.34 ± 0.25 (0.81–1.77)	1.17 ± 0.29 (0.62–1.79)	$t = 2.59$, 95% CI = 0.04, 0.31
Normal-appearing white matter	0.55 ± 0.18 (0.12–0.96)	0.63 ± 0.16 (0.35–0.96)	0.44 ± 0.14 (0.12–0.73)	$t = 5.08$, 95% CI = 0.12, 0.27
White matter hyperintensity	0.67 ± 0.28 (0.21–1.76)	0.76 ± 0.29 (0.22–1.76)	0.54 ± 0.21 (0.21–1.16)	$t = 3.64$, 95% CI = 0.10, 0.34
Phase contrast MRI				
Arterial pulsatility index	1.25 ± 0.35 (0.56–2.90)	1.23 ± 0.41 (0.56–2.90)	1.27 ± 0.25 (0.89–2.04)	$t = -0.54$, 95% CI = -0.19, 0.11
Superior sagittal sinus pulsatility index	0.47 ± 0.18 (0.10–0.95)	0.51 ± 0.18 (0.21–0.95)	0.41 ± 0.15 (0.10–0.76)	$t = 2.54$, 95% CI = 0.02, 0.17
Cerebrospinal fluid stroke volume at foramen magnum (ml)	0.57 ± 0.24 (0.10–1.64)	0.59 ± 0.28 (0.10–1.64)	0.55 ± 0.20 (0.11–0.85)	$t = 0.58$, 95% CI = -0.08, 0.14
Cerebrovascular reactivity (%/mmHg)				
Subcortical gray matter	0.127 ± 0.072 (-0.182–0.237)	0.132 ± 0.074 (-0.182–0.237)	0.121 ± 0.071 (-0.101–0.220)	$t = 0.65$, 95% CI = -0.024, 0.046
Normal-appearing white matter	0.035 ± 0.036 (-0.128–0.093)	0.035 ± 0.036 (-0.128–0.086)	0.035 ± 0.036 (-0.058–0.093)	$t = -0.06$, 95% CI = -0.018, 0.017
White matter hyperintensity	0.022 ± 0.071 (-0.284–0.167)	0.022 ± 0.082 (-0.284–0.167)	0.021 ± 0.056 (-0.138–0.114)	$t = 0.05$, 95% CI = -0.033, 0.034
T_1 (s)				
Subcortical gray matter	1.26 ± 0.07 (1.15–1.53)	1.25 ± 0.04 (1.19–1.36)	1.28 ± 0.08 (1.15–1.53)	$t = -2.03$, 95% CI = -0.07, -0.00
Normal-appearing white matter	0.94 ± 0.04 (0.87–1.05)	0.94 ± 0.04 (0.88–1.04)	0.95 ± 0.04 (0.87–1.05)	$t = -1.18$, 95% CI = -0.03, 0.01
White matter hyperintensity	1.35 ± 0.11 (1.14–1.75)	1.34 ± 0.12 (1.14–1.75)	1.38 ± 0.10 (1.22–1.59)	$t = -1.50$, 95% CI = -0.09, 0.01
Mean diffusivity ($10^{-3} \text{ mm}^2/\text{s}$)				
Subcortical gray matter	0.70 ± 0.08 (0.54–1.01)	0.66 ± 0.035 (0.62–0.80)	0.74 ± 0.09 (0.54–1.01)	$t = -4.68$, 95% CI = -0.11, -0.04
Normal-appearing white matter	0.65 ± 0.03 (0.58–0.70)	0.63 ± 0.03 (0.58–0.70)	0.66 ± 0.03 (0.60–0.70)	$t = -4.72$, 95% CI = -0.05, -0.02
White matter hyperintensity	0.95 ± 0.11 (0.69–1.20)	0.90 ± 0.09 (0.69–1.16)	1.02 ± 0.08 (0.87–1.20)	$t = -6.16$, 95% CI = -0.17, -0.09
Fractional anisotropy				
Subcortical gray matter	0.24 ± 0.03 (0.16–0.32)	0.25 ± 0.02 (0.20–0.32)	0.22 ± 0.030 (0.16–0.28)	$t = 4.54$, 95% CI = 0.02, 0.04
Normal-appearing white matter	0.48 ± 0.03 (0.37–0.54)	0.50 ± 0.02 (0.45–0.54)	0.46 ± 0.03 (0.37–0.51)	$t = 6.27$, 95% CI = 0.03, 0.06
White matter hyperintensity	0.31 ± 0.06 (0.20–0.42)	0.34 ± 0.04 (0.24–0.42)	0.27 ± 0.04 (0.20–0.41)	$t = 7.27$, 95% CI = 0.05, 0.09

All values reported as mean \pm standard deviation (range). Differences between CADASIL and sporadic SVD presented as t -tests: t -value and 95% confidence intervals (95% CI), unadjusted for covariates.

Abbreviations: CADASIL = cerebral autosomal dominant arteriopathy with subcortical infarcts and leukoencephalopathy; MRI = magnetic resonance imaging; SVD = small vessel disease.

Table 3. Linear Regressions with Outcome White Matter Hyperintensity Volume Log(base 10) Normalized to Intracranial Volume Against Tissue-Specific Predictors

Outcome	Log ₁₀ (WMH volume/intracranial volume)		
Tissue-specific predictors in NAWM			
Predictor	<i>B</i>	95% CI	<i>p</i> value
Intercept	−2.73	−3.47 to −1.99	<0.0001
Age	0.0134	0.0032–0.0236	0.011
Smoker	0.102	−0.086–0.289	0.28
PS (×10,000)	0.020	−0.087–0.126	0.71
CVR	−1.72	−4.65–1.20	0.24
CADASIL vs sporadic	0.99	0.76–1.22	<0.0001
Systolic BP variability	−6.44	−11.2 to −1.72	0.0084
Venous pulsatility index	0.224	−0.487–0.936	0.53
Plasma volume (<i>v_p</i> , ×100)	−0.589	−1.19–0.01	0.054
Arterial pulsatility index	0.116	−0.154–0.386	0.39
Tissue-specific predictors in WMH			
Intercept	−2.6	−3.3 to −1.9	<0.0001
Age	0.0104	−0.000 –0.0203	0.041
Smoker	0.096	−0.080–0.272	0.28
PS (×10,000)	0.010	−0.07 –0.095	0.82
CVR	−1.78	−3.30 to −0.27	0.02
CADASIL vs sporadic	0.98	0.78–1.19	<0.0001
Systolic BP variability	−5.00	−9.37 to −0.63	0.026
Venous pulsatility index	0.116	−0.567–0.799	0.73
Plasma volume (<i>v_p</i> , ×100)	−0.594	−0.987 to −0.202	0.0037
Arterial pulsatility index	0.119	−0.127–0.365	0.34

Tissue-specific predictors include permeability surface area product (PS), cerebrovascular reactivity (CVR), blood plasma volume (v_p) in normal-appearing white matter (NAWM) or WMH using separate models, venous pulsatility index and adjusted for key vascular risk factors. All results are reported as unstandardized *B* value, 95% confidence interval (95% CI), and *p* value. In separate models, v_p was substituted for permeability surface area product (PS), and arterial pulsatility index for venous pulsatility index as the variables were derived from the same data source and to avoid over-specifying the model.

CADASIL, cerebral autosomal dominant arteriopathy with subcortical infarcts and leukoencephalopathy; WMH = white matter hyperintensity.

We found the vascular functions differed more between NAWM and WMH than between SVD subtypes (Table 4). For example, CVR did not differ between CADASIL and sporadic SVD patients ($B = 0.0169$, 95% CI -0.0247 , 0.0584 , $p = 0.42$), but was lower in WMH than in NAWM ($B = -0.048$, 95% CI -0.079 , -0.017 , $p = 0.0033$). Indeed, there were interactions between WMH volume and tissue type such that the worse the

WMH volume the steeper the difference in v_p and CVR between NAWM and WMH (Table 4, Fig 3). Furthermore, the association with tissue damage was such that in both tissues, patients with larger WMH volumes had lower CVR (NAWM: $B = -0.023$, 95% CI -0.055 , 0.010 , $p = 0.17$; WMH: $B = -0.044$, 95% CI -0.077 , -0.011 , $p = 0.01$), lower v_p (NAWM: $B = -0.00129$, 95% CI -0.00250 , -0.00008 , $p = 0.0037$; WMH:

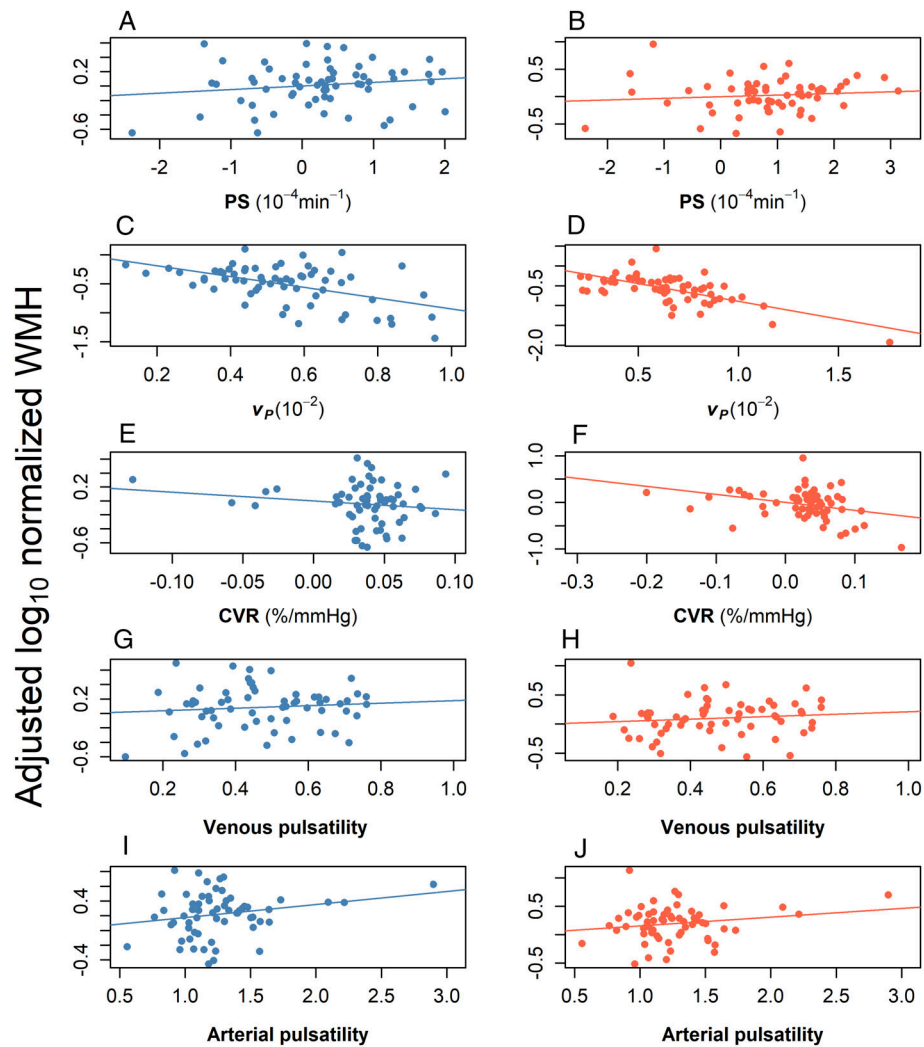


Figure 2: Graphs showing regression lines (see Table 3 for details of coefficients) showing \log_{10} normalized white matter hyperintensity (WMH) volume, adjusted for age, smoking status, systolic blood pressure, and the remaining imaging variables against each tissue/vascular function in normal-appearing white matter (blue, left) and WMH (red, right) for (A, B) permeability surface area product (PS); (C, D) blood plasma volume (v_P); (E, F) cerebrovascular reactivity (CVR); (G, H) venous pulsatility; and (I, J) arterial pulsatility. Blood plasma volume fraction (v_P) was substituted for PS, and arterial pulsatility for venous pulsatility in separate models, as the variables were derived from the same data source or were collinear, and to avoid overspecifying the model.

$B = -0.00218$, 95% CI -0.00344 , -0.00091 , $p = 0.0011$), and a tendency to higher PS (NAWM: $B = 0.154$, 95% CI -0.551 , 0.859 , $p = 0.66$; WMH: $B = 0.106$, 95% CI -0.621 , 0.834 , $p = 0.77$).

Relationships Between Vascular Functions

We found only nominal associations between most vascular function metrics. PS tended to be higher in patients with lower CVR ($B = -0.85$, 95% CI -4.72 , 3.02 , $p = 0.66$), higher venous pulsatility ($B = 1.23$, 95% CI -0.57 , 3.03 , $p = 0.18$), and lower arterial pulsatility ($B = -0.084$, 95% CI -0.780 , 0.612 , $p = 0.81$) (Table 4 and S7). v_P tended to be higher in patients with lower PS ($B = -0.0050$, 95% CI -0.0416 , 0.0317 , $p = 0.79$),

lower venous pulsatility ($B = -0.180$, 95% CI -0.484 , 0.00124 , $p = 0.24$), lower arterial pulsatility ($B = -0.094$, 95% CI -0.207 , 0.018 , $p = 0.099$), and higher CVR ($B = 0.89$, 95% CI 0.12 , 1.66 , $p = 0.024$). CVR tended to be higher in patients with higher venous ($B = 0.077$, 95% CI -0.006 , 0.160 , $p = 0.068$) and lower arterial ($B = -0.0007$, 95% CI -0.0335 , 0.0321 , $p = 0.97$) pulsatility.

Main Sources of Variability in SVD

In the PCA including all patients (Fig 4a), the highest proportion of variance was explained by a factor representing WMH volume, WMH T_1 , FA, and MD. The remaining factors, in decreasing order of variance

Table 4. Linear Mixed Models with Tissue-Based Vascular Functions Measured in Normal-Appearing White Matter and White Matter Hyperintensities as Outcome Adjusting for the Remaining Vascular Functions and Key Covariates.

	Outcome	Predictor	<i>B</i>	95% CI	<i>p</i> value
(a)	PS	Intercept	0.47	−2.18–3.11	0.73
		Age	−0.0151	−0.0426–0.0124	0.28
		Smoker	−0.134	−0.618–0.350	0.58
		log ₁₀ (WMH vol/ICV)	0.154	−0.551–0.859	0.66
		Venous pulsatility index	1.23	−0.57–3.03	0.18
		CADASIL vs sporadic	0.042	−0.858–0.943	0.93
		Systolic BP variability	6.2	−6.3–18.6	0.32
		CVR	−0.85	−4.72–3.02	0.66
		Tissue type (WMH vs NAWM)	0.46	−0.18–1.10	0.16
		log ₁₀ (WMH vol/ICV) × tissue type	−0.047	−0.371–0.276	0.77
(b)	<i>v_p</i>	Intercept	0.014	−0.430 – 0.458	0.95
		Age	0.00269	−0.00193–0.00731	0.25
		Smoker	−0.0067	−0.0874–0.074	0.87
		log ₁₀ (WMH vol/ICV)	−0.129	−0.250 to −0.008	0.037
		Venous pulsatility index	−0.180	−0.484–0.124	0.24
		CADASIL vs sporadic	0.018	−0.133–0.168	0.81
		Systolic BP variability	2.34	0.26–4.43	0.028
		PS (×10,000)	−0.0050	−0.0416–0.0317	0.79
		CVR	0.89	0.12–1.66	0.024
		Tissue type (WMH vs NAWM)	−0.042	−0.197–0.113	0.59
(c)	CVR	Intercept	0.05	−0.07–0.17	0.40
		Age	−0.0011	−0.0023–0.0002	0.096
		Smoker	−0.006	−0.029–0.016	0.57
		log ₁₀ (WMH vol/ICV)	−0.023	−0.055–0.010	0.17
		Venous pulsatility index	0.077	−0.006–0.160	0.068
		CADASIL vs Sporadic	0.0169	−0.0247–0.0584	0.42
		Systolic BP variability	−0.5	−1.0–0.1	0.10
		PS (×10,000)	−0.0015	−0.0106–0.0075	0.73
		Tissue type (WMH vs NAWM)	−0.048	−0.079 to −0.017	0.0033
		log ₁₀ (WMH vol/ICV) × tissue type	−0.021	−0.037 to −0.005	0.011

All results are reported as unstandardized *B* value, 95% confidence interval (95% CI), and *p* value. In separate models, and arterial pulsatility index for venous pulsatility index as the variables were derived from the same data source and to avoid overspecifying the model.

CVR = cerebrovascular reactivity; ICV = intracranial volume; vol = volume.

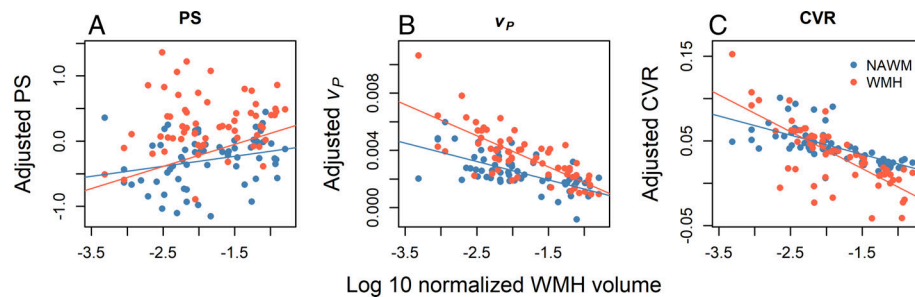


Figure 3: Graphs showing the interaction between vascular functions adjusted for age, smoking status, systolic blood pressure variability, tissue type (normal appearing white matter [NAWM, blue] and white matter hyperintensities [WMH; red]), and the remaining vascular functions against WMH volume. (A) Permeability surface area product (PS); (B) blood plasma volume (v_P)*, and (C) cerebrovascular reactivity (CVR)*. See Table 4 for coefficients. *Conventionally significant interaction ($p \leq 0.05$) between WMH and tissue-of-interest (NAWM or WMH).

explained, were venous pulsatility and age; arterial pulsatility; WMH v_P , NAWM FA, MD, and v_P ; BPV; WMH and NAWM CVR; and number of microbleeds.

The factor order and explained variance differed between disease subtypes. In patients with CADASIL (Fig 4b), a factor representing NAWM FA, WMH T_1 , FA, and MD explained the most variance, followed by age; PVS score; venous pulsatility; NAWM and WMH CVR; BPV; WMH and NAWM PS; and arterial pulsatility. In patients with sporadic SVD (Fig 4c), a factor representing arterial pulsatility explained most variance, followed by venous pulsatility; WMH and NAWM PS; BPV; number of microbleeds; WMH FA, MD, and T_1 ; and NAWM T_1 . In general, FA/MD explained less variance in sporadic SVD patients than in either the whole group or CADASIL patients. Of the vascular function measures, more variance was explained by CVR in CADASIL patients and PS in sporadic SVD patients, whereas venous and/or arterial pulsatility explained a similar amount in both subtypes.

Discussion

In this international, multicenter study, thought to be the first such, we concurrently assessed 3 key vascular functions—BBB leakage, blood pulsatility and CVR, and structural brain damage—in patients with sporadic and genetic SVD. We found more severe SVD was associated with worse vascular function in sporadic SVD and CADASIL patients. Tissue type (ie, NAWM/WMH) generally more strongly predicted vascular function differences than SVD subtype. Despite SVD subtypes differing in clinical presentation, disease severity and presumed pathogenesis underlying vascular functions and tissue structural changes were similar. However, the 3 vascular functions were generally not closely interrelated, suggesting that although all 3 functions may contribute to SVD

pathogenesis, they may do so at different stages in lesion development.^{32,33} We also showed the feasibility of assessing 3 complex vascular functions concurrently in a multicenter MRI study, and provided a robust protocol for use as intermediary outcomes in future clinical trials testing potential SVD treatments.¹⁸

Associations Between Disease Burden and Vascular Function Metrics

Consistent with previous single-center studies testing individual vascular functions in 1 SVD subtype (not all covariate adjusted), we found patients with higher WMH burden tended to have higher BBB leakage,^{10,34} and arterial and venous pulsatility,⁹ but lower v_P ³⁴ and CVR^{12,35} in NAWM and WMH. Mirroring our findings, several studies reported higher BBB leakage in patients with more severe WMH^{6,10}; higher WMH burden has generally been linked to higher PS and lower v_P in sporadic SVD.^{6,34} Higher arterial and venous PC-MRI pulsatility was associated with higher WMH burden in sporadic SVD,^{9,36} and patients with CADASIL had higher arterial transcranial Doppler pulsatility than healthy controls.³⁷ Lower CVR was linked to higher WMH burden in both sporadic SVD¹² and CADASIL patients,³⁸ consistent with recent 7-T studies.^{39,40}

Associations Between SVD Subtype and Vascular Functions

Despite higher WMH severity in CADASIL patients, we found negligible evidence that vascular functions differed between SVD subtypes adjusting for key covariates, disease severity, and tissue type. Few previous studies included sporadic SVD and CADASIL patients. One found higher BBB leakage than healthy controls in patients with sporadic SVD patients, but not CADASIL patients (all $n = 20$)¹¹; but did not report v_P , correct for scanner drift, and controls were older, despite age being

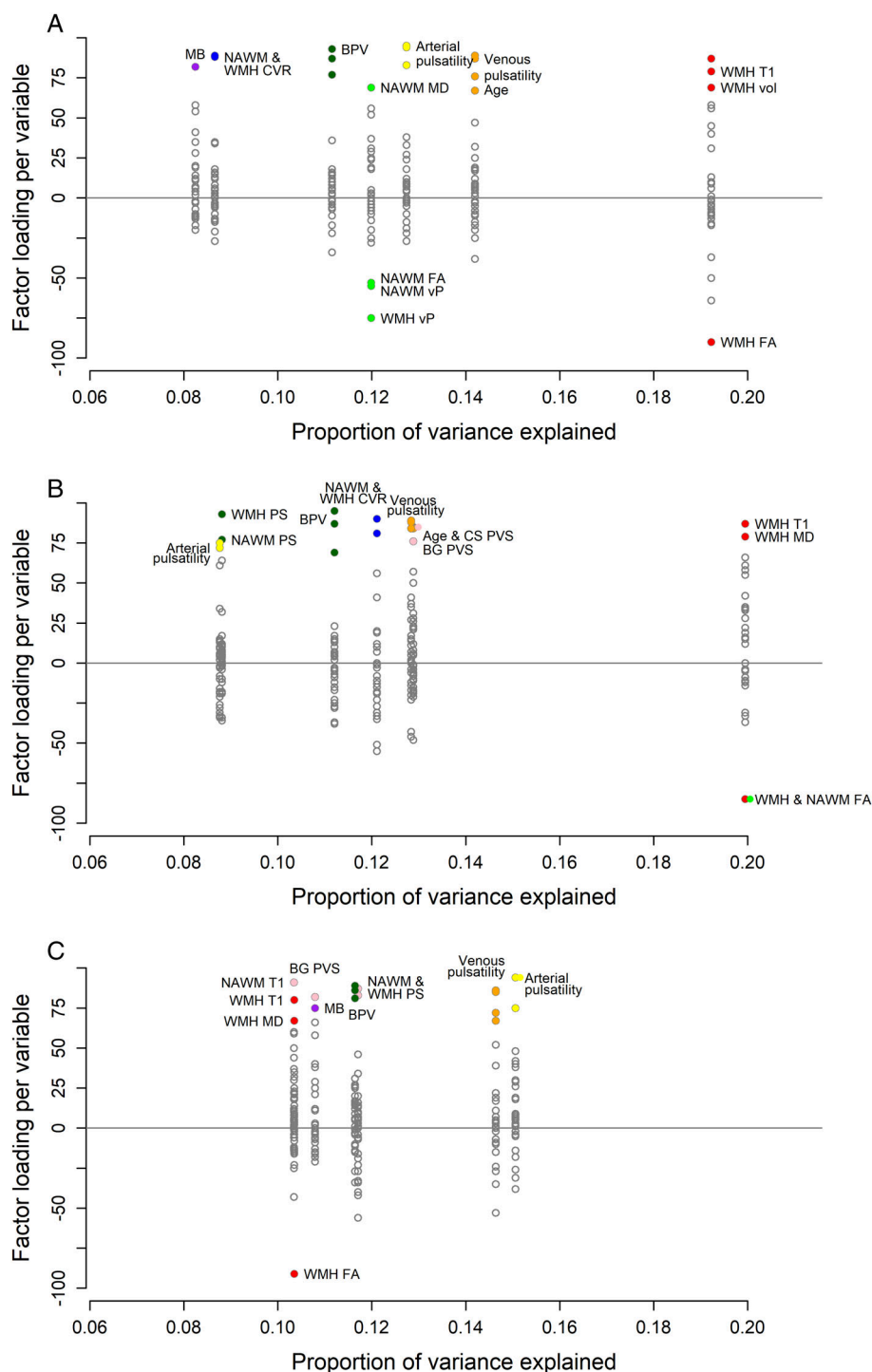


Figure 4: Principal component analysis. Factor loadings for each variable (y-axis) versus variance in the data explained by each component for (A) all patients together, (B) cerebral autosomal dominant arteriopathy with subcortical infarcts and leukoencephalopathy only, and (C) sporadic small vessel diseases only (x-axis). The labels describe the variables included in each factor. Color of variables reflects their original component in the “all patient” principal components analysis. BG = basal ganglia; BPV, blood pressure variability; CS = centrum semiovale; FA = fractional anisotropy; MB = microbleed; MD = mean diffusivity; NAWM = normal appearing white matter; PS = blood–brain barrier leakage (permeability surface area); PVS = perivascular space score; v_P = blood plasma volume; WMH = white matter hyperintensity volume.

associated with higher BBB leakage.⁴¹ Although higher BBB leakage was not found in transgenic CADASIL mouse models,⁴² patient cerebrospinal fluid/serum

albumin ratio was elevated ($n = 89$).⁴³ Basal ganglia regions with perivascular iron accumulation had higher BBB leakage in symptomatic/asymptomatic CADASIL

patients ($n = 10/11$) than controls.⁴⁴ In CADASIL patients, higher fibrinogen extravasation was reported on histopathology in WMH around enlarged PVS and lacunes,⁴² a sign of BBB leakage. In unadjusted analysis, no CVR differences were found between patients with CADASIL ($n = 10$) versus sporadic SVD with moderate/severe WMH ($n = 20/12$).⁴⁵

PS differences between CADASIL and sporadic SVD patients may suggest PS increases occur earlier, whereas CVR reduction could become the dominant function in established severe disease. However, underlying v_p and vascular surface area differences may contribute.³⁴ Together with reported regional differences in WMH characteristics,^{46,47} spatially localized analysis methods³² and larger samples size are needed to investigate how BBB function varies between, and within, SVD subtypes and tissues.

Similarities and Differences between NAWM and WMH with Increasing WMH Volume

Lower CVR and v_p were more strongly associated with higher WMH burden in WMH than NAWM. Few studies measured WMH CVR,^{8,35,39} although CVR was lower in WMH than NAWM, and, in 1 study, NAWM evolved into WMH at 1 year.¹³ Although some studies found stronger associations between PS, v_p and disease burden in NAWM than WMH,^{34,48} others reported stronger associations in WMH.⁴⁹ As PS combines permeability and vascular surface area, microvessel density decreases complicate interpretation; for example, in damaged tissue, partly reflected here in lower v_p in WMH and consistent with steeper v_p decline with higher WMH burden in WMH than NAWM.³⁴ Given microvessels are likely to be sparse in patients with severe WMH seen in CADASIL, indicated by lower v_p , true brain microvessel permeability is likely much higher than reflected by measured PS.⁵⁰ Several factors, including patient population, sample size, methodology, and disease stage, potentially associated with higher/lower disease burdens or more/less acute effects, may also contribute.^{6,34}

Relationships Between Different Vascular Functions

We did not generally find strong interrelationships between different vascular functions, as reflected in the often broad confidence intervals, only associations between higher v_p and higher CVR reached conventional significance, whereas CVR trended higher with venous pulsatility. However, the directions of effects agree with our initial hypotheses; for example, patients with higher PS tended to have higher venous pulsatility and lower CVR.

Although cross-sectional, the present findings suggest only limited overlap between different functions, as reflected in the PCA results. Therefore, each vascular function may have a complementary role, possibly differing in order of occurrence in SVD pathogenesis. We are not able to determine the time order of vascular functions in this cross-sectional study, but considering the disease severity associations, we could speculate that BBB leakage increases early,^{11,32} followed by increases in pulsatility, decline in CVR, and v_p as damage accumulates. Future studies should assess longitudinal associations between vascular function metrics and tissue changes.

Principal Component Analysis

The PCA showed that although WMH volume and quantitative tissue microstructural metrics explained the most variance in all patients and CADASIL patients, arterial pulsatility explained most variance in sporadic SVD. Venous pulsatility explained similar amounts of variance in all 3 analyses; however, arterial pulsatility explained less variance in CADASIL patients. CVR explained more variance in CADASIL patients and PS in sporadic SVD patients. As CADASIL is a more extreme SVD phenotype, differences may result from more advanced disease¹ and, potentially, exhaustion of compensatory vascular processes. However, longitudinal replication is required to draw concrete conclusions, as the subtype analyses were exploratory.

Strengths/Limitations

The strengths of this study included concurrent assessment of multiple vascular functions in patients with two SVD subtypes, multicenter recruitment, rigorous data acquisition, processing, and quality assurance,^{7,9,14,19,20} following consensus recommendations⁶ and best practice.⁸ We reduced artifacts and tissue signal contamination while maximizing tissue inclusion for vascular functions and quantitative measures. We demonstrated the feasibility of using these complex MRI measures in a multicenter study (>90% of patients provided usable data), demonstrating they can be used as intermediary outcomes in clinical trials of interventions in SVD.¹⁸ We assessed relationships between variables by interpreting findings in the context of direction of effect, confidence interval breadth, and existing clinical knowledge, rather than solely p values.^{29,30}

Limitations included shortcomings of existing methods to measure vascular function in vivo. Although we used an established well-validated approach, BOLD-MRI only indirectly measures blood flow and cerebral blood volume but other factors contribute to BOLD signal changes.^{8,51} However, response to 6% CO₂ reflects

capillary, as well as arteriolar dilation.⁵² Susceptibility artifact and patient motion may confound accurate CVR measurement, although we were careful to minimize artifacts. DCE-MRI measurements of BBB leakage are limited by the low-level permeability changes and background noise, likely contributing to the broader confidence intervals in some analyses involving BBB leakage. However, DCE-MRI remains the consensus technique for measuring subtle BBB leakage.⁶ Whereas an established technique, 2D PC-MRI has limited field of view, and anatomical variability can make image plane positioning challenging,⁹ although we adopted a harmonized imaging protocol. For dMRI, we used an established method²⁷ using all available data (Supplementary material); however, alternative, more advanced (although less widely validated) approaches exist,⁵³ which could be explored in future. As a hypothesis-generating work, we refer to the direction of effect, even where broad confidence intervals indicate limited confidence, further methodological development may help refine these estimates. The present findings also provide the first data for a multicenter analysis of 3 vascular dysfunction measures, providing a basis for meaningful sample size calculations for similar studies in future. The long imaging protocol may bias recruitment to more physically able patients. Due to recruitment practicalities, all patients with CADASIL were recruited at a single site, with no repeat scanning of the same patients, and a separate “healthy” control group was not acquired, as healthy controls do not account for medication, co-existing conditions, and SVD prevalence in “normal” aging, adding little to the study design.¹ However, scans were acquired on 3-T scanners from one vendor, and sites conducted routine quality assurance volunteer and phantom assessments (Supplementary material).¹⁴ Inherent differences in tissue volumes between patients with sporadic SVD and CADASIL may influence results; for example, WMH volumes were generally larger and NAWM smaller in CADASIL patients than sporadic SVD patients. More diffuse and smaller clusters of tissue are more susceptible to partial volume effect, potentially influencing measurements, particularly in uneroded WMH. Although SGM and NAWM were eroded to minimize contamination, we maximized the amount of included tissue. Due to the limited sample size, we did not evaluate interaction terms for vascular function measures and SVD subtype, nor associations with sex.

Longitudinal studies are required to determine if different vascular functions predominate at different stages of disease, and how each function contributes to SVD lesions. Further translational research and histological validation is needed to better understand hemodynamic measures and their interdependencies,⁵⁰ and whether vascular function can be improved with interventions.¹⁸

Conclusion

We showed that 3 vascular function mechanisms (BBB leakage, CVR, and blood pulsatility) occur in both CADASIL and sporadic SVD patients, are all associated with WMH severity, and differ between WMH/NAWM. Associations between different vascular functions and SVD burden suggest a complex, sequential process. Despite stark differences in visible SVD burden, similar vascular functions are implicated in both SVD subtypes. Although inferences on vascular function evolution from this cross-sectional study are limited, the association analysis and PCA may suggest differential evolution, with BBB leakage increasing early, followed by increased pulsatility, and declining CVR and v_p as microvascular and tissue damage accumulates. Finally, we showed that complementary sophisticated vascular functions measures can be assessed in multicenter SVD studies with minimal data loss, providing intermediary outcome measures for clinical trials and observational studies.

Acknowledgments

European Union Horizon 2020 (project No 666881, “SVDs at target”). Additional support is provided by the Stroke Association Postdoctoral Fellowship (SA PDF 23 \100007, MSS) and Princess Margaret Research Development Fellowship scheme (GWB), Alzheimer’s Society (Ref: 252(AS-PG-14-033), GWB), Age UK and Biotechnology and Biological Sciences Research Council (BB/W008793/1) (SMM), Wellcome Trust (Grant number: 224912/Z/21/Z; Translational Neuroscience PhD programme at the University of Edinburgh, DJG), Stroke Association Garfield Weston Foundation Senior Clinical Lectureship (SA LECT 2015/04, FND), NHS Research Scotland (FND), Chief Scientist Office (CAF/18/08, UC), NHS Lothian Research and Development Office (MJT), the Row Fogo Charitable Trust, the Scottish Funding Council through the Scottish Imaging Network, and A Platform for Scientific Excellence (SINAPSE) Collaboration. Funding is gratefully acknowledged from Foundation Leducq (ref no. 16 CVD 05), Lothians Health Foundation, and MRC UK Dementia Research Institute (funded by the MRC, Alzheimer’s Society and Alzheimer’s Research UK). Further support is provided by the Vascular Dementia Research Foundation and German Research Foundation (DFG) as part of the Munich Cluster for Systems Neurology (EXC 2145 SyNergy–D 390857198). The procurement of the MRI scanner in Munich was supported by the DFG grant for major research instrumentation (DFG, INST 409/193-1 FUGG). We thank the radiographers for helping

implement the imaging protocol and scanning, Dr Alastair Webb and Professor Martin Middeke for advice on selecting the optimal BP variable and BP data processing, and the patients for participating.

Author Contributions

J.M.W., M.Di., G.J.B., and R.v.O. contributed to the conception and design of the study; M.S.S., G.W.B., A.K., D.K., M.J.T., F.M.C., S.M.M., R.B., K.S., I.H., D.J.G., F.N.D., U.C., E.S., T.P., E.J., M.Du., M.I., J.S., W.H.B., and members of the SVDs@Target consortium contributed to the acquisition and analysis of data; M.S.S., M.J.T., F.M.C., and J.M.W. contributed to drafting the text or preparing the figures.

Potential Conflicts of Interest

Nothing to report.

Data Availability

The study data are available from the SVDs@target collaborative group via the corresponding author, upon reasonable request.

References

- Wardlaw JM, Smith C, Dichgans M. Small vessel disease: mechanisms and clinical implications. *Lancet Neurology* 2019;18:684–696.
- Debette S, Schilling S, Duperron MG, et al. Clinical significance of magnetic resonance imaging markers of vascular brain injury: a systematic review and meta-analysis. *JAMA Neurol* 2019;76:81–94.
- Ma Y, Yilmaz P, Bos D, et al. Blood pressure variation and subclinical brain disease. *J Am Coll Cardiol* 2020;75:2387–2399.
- Wardlaw JM, Debette S, Jokinen H, et al. ESO guideline on covert cerebral small vessel disease. *Eur Stroke J* 2021;6:4.
- Wardlaw JM, Smith EE, Biessels GJ, et al. Neuroimaging standards for research into small vessel disease and its contribution to ageing and neurodegeneration. *Lancet Neurol* 2013;12:822–838.
- Thrippleton MJ, Backes WH, Sourbron S, et al. Quantifying blood-brain barrier leakage in small vessel disease: review and consensus recommendations. *Alzheimers Dement* 2019;15:840–858.
- Thrippleton MJ, Shi Y, Blair G, et al. Cerebrovascular reactivity measurement in small vessel disease: rationale and reproducibility of a protocol for MRI acquisition and image processing. *Int J Stroke* 2018;13:195–206.
- Sleight E, Stringer MS, Marshall I, et al. Cerebrovascular reactivity measurement using magnetic resonance imaging: a systematic review. *Front Physiol* 2021;12:643468.
- Shi Y, Thrippleton MJ, Blair GW, et al. Small vessel disease is associated with altered cerebrovascular pulsatility but not resting cerebral blood flow. *J Cereb Blood Flow Metab* 2020;40:85–99.
- Wardlaw JM, Makin SJ, Valdés Hernández MC, et al. Blood-brain barrier failure as a core mechanism in cerebral small vessel disease and dementia: evidence from a cohort study. *Alzheimers Dement* 2017;13:634–643.
- Walsh J, Tozer DJ, Sari H, et al. Microglial activation and blood-brain barrier permeability in cerebral small vessel disease. *Brain* 2021;144:1361–1371.
- Blair GW, Thrippleton MJ, Shi Y, et al. Intracranial hemodynamic relationships in patients with cerebral small vessel disease. *Neurology* 2020;94:e2258–e2269.
- Sam K, Conklin J, Holmes KR, et al. Impaired dynamic cerebrovascular response to hypercapnia predicts development of white matter hyperintensities. *Neuroimage Clin* 2016;11:796–801.
- Blair GW, Stringer MS, Thrippleton MJ, et al. Imaging neurovascular, endothelial and structural integrity in preparation to treat small vessel diseases. The INVESTIGATE-SVDs study protocol. Part of the SVDs@Target project. *Cereb Circ Cogn Behav* 2021;2:100020.
- Reshetnik A, Gohlisch C, Zidek W, et al. Validation of the Tel-O-GRAPH, a new oscillometric blood pressure-measuring device, according to the British hypertension society protocol. *Blood Press Monit* 2016;21:307–309.
- Webb AJ, Rothwell PM. Physiological correlates of beat-to-beat, ambulatory, and day-to-day home blood pressure variability after transient ischemic attack or minor stroke. *Stroke* 2014;45:533–538.
- Rothwell PM. Limitations of the usual blood-pressure hypothesis and importance of variability, instability, and episodic hypertension. *Lancet* 2010;375:938–948.
- Kopczak A, Stringer MS, van den Brink H, et al. Effect of blood pressure-lowering agents on microvascular function in people with small vessel diseases (TREAT-SVDs): a multicentre, open-label, randomised, crossover trial. *Lancet Neurol* 2023;22:991–1004.
- Thrippleton MJ, Blair GW, Valdes-Hernandez MC, et al. MRI relaxometry for quantitative analysis of USPIO uptake in cerebral small vessel disease. *Int J Mol Sci* 2019;20(3):776.
- Manning C, Stringer M, Dickie B, et al. Sources of systematic error in DCE-MRI estimation of low-level blood-brain barrier leakage. *Magn Reson Med* 2021;86:1888–1903.
- Fazekas F, Chawluk JB, Alavi A, et al. MR signal abnormalities at 1.5 T in Alzheimer's dementia and normal aging. *AJR Am J Roentgenol* 1987;149:351–356.
- Farrell C, Chappell F, Armitage PA, et al. Development and initial testing of normal reference MR images for the brain at ages 65–70 and 75–80 years. *Eur Radiol* 2009;19:177–183.
- Jenkinson M, Bannister P, Brady M, Smith S. Improved optimization for the robust and accurate linear registration and motion correction of brain images. *NeuroImage* 2002;17:825–841.
- Smith SM. Fast robust automated brain extraction. *Hum Brain Mapp* 2002;17:143–155.
- Patenaude B, Smith SM, Kennedy DN, Jenkinson M. A Bayesian model of shape and appearance for subcortical brain segmentation. *NeuroImage* 2011;56:907–922.
- Zhang Y, Brady M, Smith S. Segmentation of brain MR images through a hidden Markov random field model and the expectation-maximization algorithm. *IEEE Trans Med Imaging* 2001;20:45–57.
- Clayden JD, Maniega SM, Storkey AJ, et al. TractoR: magnetic resonance imaging and tractography with R. *J Stat Softw* 2011;44:1–18.
- Babyak MA. What you see may not be what you get: a brief, nontechnical introduction to overfitting in regression-type models. *Psychosom Med* 2004;66:411–421.
- Wasserstein RL, Lazar NA. The ASA's statement on p-values: context, process, and purpose. *Am Stat* 2016;70:129–131.
- Wasserstein RL, Schirm AL, Lazar NA. Moving to a world beyond “ $p < 0.05$ ”. *Am Stat* 2019;73:1–19.
- Sainani KL. Introduction to principal components analysis. *PM R* 2014;6:275–278.
- Rudilosso S, Stringer MS, Thrippleton M, et al. Blood-brain barrier leakage hotspots collocating with brain lesions due to sporadic and monogenic small vessel disease. *J Cereb Blood Flow Metab* 2023;43:1490–1502.

33. Rudilosso S, Chui E, Stringer MS, et al. Prevalence and significance of the vessel-cluster sign on susceptibility-weighted imaging in patients with severe small vessel disease. *Neurology* 2022;99:e440–e452.
34. Stringer MS, Heye AK, Armitage PA, et al. Tracer kinetic assessment of blood-brain barrier leakage and blood volume in cerebral small vessel disease: associations with disease burden and vascular risk factors. *Neuroimage Clin* 2021;32:102883.
35. Sleight E, Stringer MS, Clancy U, et al. Cerebrovascular reactivity in patients with small vessel disease: a cross-sectional study. *Stroke* 2023;54:2776–2784.
36. Shi Y, Thrippleton MJ, Marshall I, Wardlaw JM. Intracranial pulsatility in patients with cerebral small vessel disease: a systematic review. *Clin Sci (Lond)* 2018;132:157–171.
37. Peters N, Freilinger T, Opherk C, et al. Enhanced L-arginine-induced vasoreactivity suggests endothelial dysfunction in CADASIL. *J Neurol* 2008;255:1203–1208.
38. Liem MK, Lesnik Oberstein SA, Haan J, et al. Cerebrovascular reactivity is a main determinant of white matter hyperintensity progression in CADASIL. *AJNR Am J Neuroradiol* 2009;30:1244–1247.
39. van den Brink H, Kopczak A, Arts T, et al. CADASIL affects multiple aspects of cerebral small vessel function on 7T-MRI. *Ann Neurol* 2023;93:29–39.
40. Van Den Brink H, Pham S, Siero JC, et al. Assessment of small vessel function using 7T MRI in patients with sporadic cerebral small vessel disease. *Neurology* 2024;102:e209136.
41. Verheggen ICM, de Jong JJA, van Boxtel MPJ, et al. Increase in blood-brain barrier leakage in healthy, older adults. *Geroscience* 2020;42:1183–1193.
42. Rajani RM, Ratelade J, Domenga-Denier V, et al. Blood brain barrier leakage is not a consistent feature of white matter lesions in CADASIL. *Acta Neuropathol Commun* 2019;7:187.
43. Dichgans M, Wick M, Gasser T. Cerebrospinal fluid findings in CADASIL. *Neurology* 1999;53:233.
44. Uchida Y, Kan H, Sakurai K, et al. Iron leakage owing to blood-brain barrier disruption in small vessel disease CADASIL. *Neurology* 2020;95:e1188–e1198.
45. Atwi S, Shao H, Crane DE, et al. BOLD-based cerebrovascular reactivity vascular transfer function isolates amplitude and timing responses to better characterize cerebral small vessel disease. *NMR Biomed* 2019;32:e4064.
46. Duchesnay E, Hadj Seleem F, De Guio F, et al. Different types of white matter hyperintensities in CADASIL. *Front Neurol* 2018;9:526.
47. De Guio F, Vignaud A, Chabriet H, Jouvent E. Different types of white matter hyperintensities in CADASIL: insights from 7-tesla MRI. *J Cereb Blood Flow Metab* 2018;38:1654–1663.
48. Zhang CE, Wong SM, van de Haar HJ, et al. Blood-brain barrier leakage is more widespread in patients with cerebral small vessel disease. *Neurology* 2017;88:426–432.
49. van de Haar HJ, Burgmans S, Jansen JF, et al. Blood-brain barrier leakage in patients with early Alzheimer disease. *Radiology* 2016;281:527–535.
50. Stringer MS, Lee H, Huuskonen MT, et al. A review of translational magnetic resonance imaging in human and rodent experimental models of small vessel disease. *Transl Stroke Res* 2021;12:15–30.
51. Liu P, De Vis JB, Lu H. Cerebrovascular reactivity (CVR) MRI with CO₂ challenge: a technical review. *NeuroImage* 2019;187:104–115.
52. Duan A, Bedgood PA, Metha AB, Bui BV. Reactivity in the human retinal microvasculature measured during acute gas breathing provocations. *Sci Rep* 2017;7:2113.
53. Duering M, Finsterwalder S, Baykara E, et al. Free water determines diffusion alterations and clinical status in cerebral small vessel disease. *Alzheimers Dement* 2018;14:764–774.